Fine Structure of Ultraviolet Photoluminescence of Tin Oxide Nanowires

B. Liu, C. W. Cheng, R. Chen, Z. X. Shen, H. J. Fan, and H. D. Sun*

Division of Physics and Applied Physics, School of Physical and Mathematical Sciences, Nanyang Technological University, 637371, Singapore

Photoluminescence (PL) properties of tin oxide (SnO_2) nanowires are studied in detail using high spectral resolution spectroscopy in a temperature range of 10–300 K. The nanowires have an average diameter of 86 nm. The high quality of the nanowires enables the observation of rich fine structures in the ultraviolet PL spectra at low temperatures. By carefully analyzing the temperature and excitation power dependent spectra, the following emissions are identified: recombination of donor–acceptor pairs, excitons bound to neutral and ionized donor impurities and optical transitions from free electrons to neutral acceptor impurities. Moreover, it is believed that the emission from recombination of free excitons is observed, which is unusual for SnO_2, a dipole forbidden direct band gap semiconductor.

Introduction

One dimensional (1D) semiconductor oxide nanorods, nanotubes, and nanowires (NWs) have attracted much attention in the past decade due to their potential applications in nanoelectronics and nanophotonics.[1–5] As a wide band gap semiconductor, SnO_2 is regarded as one of the promising materials for gas sensor, field effect transistors, solar cells, transparent electrodes, and so forth.[6–12] However, compared to the tremendous optical studies on ZnO, no effort has yet been spent on optoelectronic devices from bulk tin oxide, and there has been only rare exploration of its optical properties. The reason for this is that SnO_2 is a member of a special class of semiconductors that have direct band gaps but are dipole forbidden due to their special wave function symmetry.[13–15] However, the advance in nanostructured oxides has attracted new interest in exploiting these materials as components for nanoscale light emitting devices. Due to a quantum confinement in the reduced dimensionality, the wave function symmetry can be broken and hence the dipole forbidden selection rule can be relieved. Especially for SnO_2, the exciton binding energy is as large as 130 meV, which envisages efficient exciton emission at room temperature and even at higher temperatures. From the viewpoint of fundamental physics, investigation on the optical properties of SnO_2 NWs should be of great significance. Much effort has been paid to the fabrication of nanostructured SnO_2 by employing various techniques, such as the molten salt method, hydrothermal method, laser ablation deposition, and direct oxidation growth.[16–26] The ultraviolet (UV) emission from SnO_2 NWs obtained from different fabrication conditions or methods may exhibit different characteristics.

Previously, we have observed strong band edge emission from SnO_2 NWs with a typical diameter of about 15 nm.[27] In this work, we report the new features of the optical spectra of SnO_2 NWs fabricated under different conditions with a larger average diameter of about 86 nm, which was investigated by systematic temperature and excitation density dependent photoluminescence (PL) analysis. Fine structures in the UV region are observed and carefully assigned in the low-temperature PL spectra.

Experimental Section

Single crystalline SnO_2 NWs were prepared on silicon substrates by a vapor–liquid–solid (VLS) process. First, an ~4-nm thick Au film, which served as the catalyst for the NW growth, was deposited on the Si(100) substrates by thermal evaporation at room temperature. SnO_2 powder (Sigma Aldrich, 99.9%) and graphite powder (Sigma Aldrich, 99%) with a 1:1 weight ratio were grounded and transferred to an alumina boat. Then the Au coated Si substrates and the alumina boat were placed in a small quartz tube (diameter 15 mm, length 300 mm). The substrates were typically located 1–4 cm away from the center of the boat. This quartz tube was then placed at the center inside a quartz tube furnace. The temperature of the furnace was ramped to 1050 °C at a rate of 50 °C /min and kept at the peak temperature for 1 h under a constant flow of argon of 50 sccm and a pressure of 15 mbar. After the growth, the furnace naturally cooled down to room temperature.

The crystal structure of the as-fabricated SnO_2 NWs was characterized by X-ray powder diffraction (XRD) using a Bruker D8 Advanced Diffractometer and Cu Kα radiation. A tetragonal rutile crystal structure was identified (data not shown). Morphological characterization was performed using a JEOL JSM-6700F field emission scanning electron microscope (FESEM) and a JEOL 2100 transmission electron microscope (TEM). For PL measurement, the 325 nm line from a He–Cd laser was used as the excitation source. The PL signal was collected in a backscattering geometry, dispersed by a 750 mm monochromator, and detected by a photo multiplier tube using standard lock-in technique. The widths of the entrance and exit slits of the monochromator were set at 30 μm with which the spectral resolution is ~0.8 meV near the wavelength of 370 nm. A close-cycled helium cryostat (Advanced Research System 4K) was used to provide continuous temperature variation from 10 K to room temperature.

Results and Discussion

Figure 1a is the low-magnification SEM image showing a high output of the SnO_2 NWs. The lengths of the NWs are about several tens of micrometers. The widths of NWs were statistically measured from more than 150 NWs and are plotted in the

* To whom correspondence should be addressed. E-mail: hdsun@ntu.edu.sg.
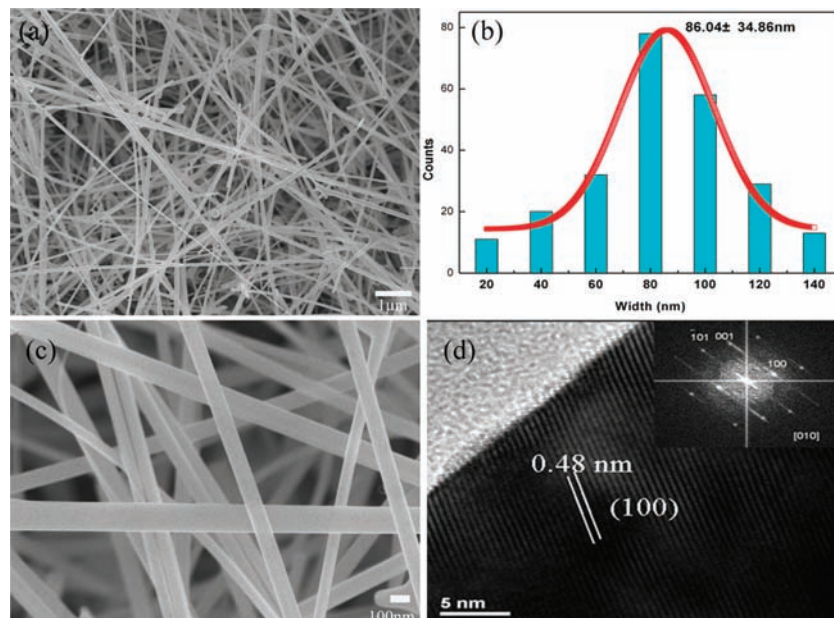
Figure 1. (a) Low-magnification SEM image of the as-synthesized SnO$_2$ nanowires. (b) A statistical distribution of the NW diameters. (c) High-magnification SEM image. (d) HRTEM lattice image. The inset shows its corresponding FFT pattern.
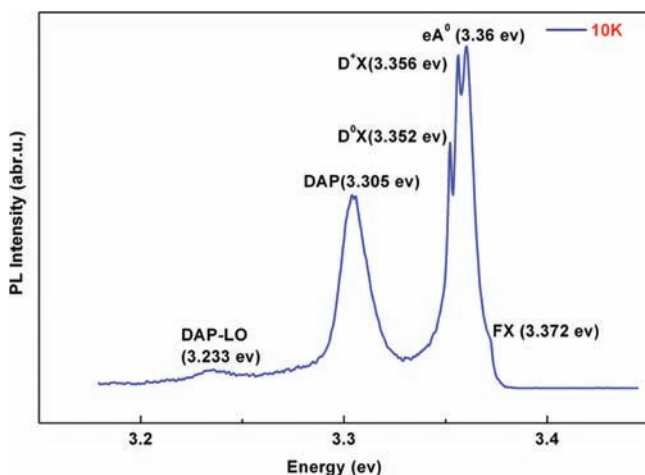

Figure 2. Ultraviolet high-resolution PL spectral of SnO$_2$ nanowires at 10K.

histogram in Figure 2b. Using a Gaussian fitting, the diameter of the NWs is about 86.04 ± 34.86 nm which is obviously larger than that of our previous samples (~15 nm). On the basis of the high-magnification SEM (Figure 1c), it is clear that the SnO$_2$ NWs have a smooth surface and regular shape. Figure 1d is the high resolution TEM (HRTEM) image of a portion of one SnO$_2$ NW. The measured d-spacing of 0.48 nm (marked with arrow) corresponds to the distance between (100) planes of the SnO$_2$ NWs. The inset of Figure 1d is a two-dimensional Fast Fourier transformation (FFT) pattern of HRTEM image, which further confirms that the SnO$_2$ NWs are single crystalline with a tetragonal rutile phase.

Figure 2 shows a typical PL spectrum of the SnO$_2$ NWs measured at 10 K in the UV wavelength range. Besides the UV emission, a broad emission band appeared at ~2.540 eV which is believed to originate from the defect states of the NWs, but will not be shown and discussed in detail in this work. Herein we focus on the UV part, which should reflect information on the exciton properties near the band edge. The UV emission consists of six distinct peaks at 3.372, 3.360, 3.356, 3.352, 3.305, and 3.233 eV whose full widths at half-maximum

(fwhm) range from 3 to 16 meV. It should be stressed that although the UV emission near 3.35 eV has been previously observed,[28] the resolved finer structure in this range has never been reported.[29,30] We attribute our observation of the fine structure to the high spectral resolution of our measurement system as well as the high sample quality in terms of crystal structure and uniformity. The two peaks at 3.360 and 3.305 eV are assigned as the recombination of band to acceptor (eA^0) and donor−acceptor pair (DAP), respectively.[15]

Further evidence of the DAP emission is given by excitation power-dependent PL measurements as shown in Figure 3. The energy of DAP luminescence can be presented by the following equation:[31] $E_g - E_D - E_A + e^2/4\pi\varepsilon r$, where E_g is the band gap energy, E_D and E_A are the donor and acceptor binding energies, respectively, e is elementary electric charge, ε is dielectric constant, and r is the donor−acceptor pair distance. With increasing excitation power, the density of photon excited donor−acceptor pairs will increase and the donor−acceptor pair distance decreases. Hence, the DAP peak will blue-shift which is indeed observed clearly in Figure 3b (red curve). The blue line in Figure 3b is the integrated PL intensity of the DAP band. It can be seen that the integrated PL intensity shows a nearly linear dependence on the laser power. This trend is also found in ZnO nanorods.[32] The energy difference between eA^0 and DAP should reflect the ionization energy of donor impurities. For our samples, the difference is 55 meV, in good agreement with the binding energy of H-donor in SnO$_2$ of 40−50 meV.[33,34] The weak band at 3.233 eV is ~72 meV lower than DAP (3.305 eV) which is close to the phonon energy of A$_{1\ g}$ mode of rutile SnO$_2$ (75 meV),[35] and therefore it can be attributed to the first-order longitudinal optical (LO) phonon replica of DAP (DAP-1LO). Higher order phonon replicas have not been observed due to the weak signal. In the Franck−Condon model, the coupling strength between the radiative transition and the LO-phonon can be characterized by the Huang−Rhys factor S.[36] The relative intensity of the nth phonon replica I_n to the zero-phonon peak I$_0$ is described by $I_n = I_0(S^n e^{-s}/n!)$, where n is a natural number. From the measured spectrum, the S factor associated with DAP is estimated to be 0.1. The S-factor in this sample is much low compared to our previously published
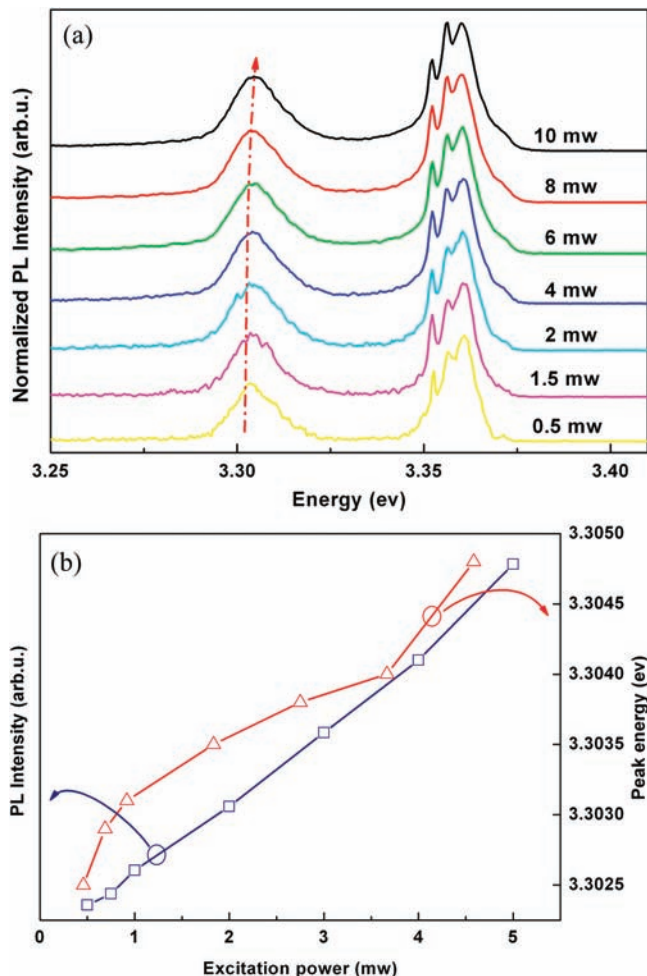
Figure 3. (a) Excitation power dependent PL spectral of SnO₂nanowires. (b) Plot of the DAP peak energy and intensity versus the excitation power.

result of SnO₂ NWs[28] in which up to three orders of LO-phonon replicas of DAP were observed and the *S* factor was 0.34. The discrepancy in *S*-factor may stem from the different NW diameters: ∼15 nm in ref.[28] while ∼86 nm for the current samples. Different NW sizes have different surface to volume ratios. The larger average diameter of NWs in this study corresponds to a smaller ratio of surface to volume and leads to a weaker exciton-LO-phonon coupling (S-factor), which is consistent with the previous report on ZnO NWs.[37]

It is noteworthy that two sharp emission peaks observed at 3.356 and 3.352 eV have never been reported previously. It is arguable that both of these two peaks originate from excitons bound to neutral (D⁰X) with different impurities, since emissions from D⁰X are very common in wide bandgap semiconductors especially at low temperatures. However, these two peaks are found to show different behaviors of the temperature evolution, indicative of their different origins. Figure 4a shows the temperature dependence of PL spectra from 10 to 300 K. We can see that the intensity of peaks at 3.352 and 3.356 eV decreases very quickly with increasing temperature and become irresolvable above 60 and 80 K, respectively. At higher temperatures, they merge with eA⁰. However, a careful inspection reveals that the temperature quenching of the peak at 3.352 eV is faster than the peak at 3.356 eV. If both peaks are from D⁰X, then the peak with a lower energy (larger binding energy) should have larger thermal activation energy and demonstrates slower temperature quenching. Therefore, we attribute these two
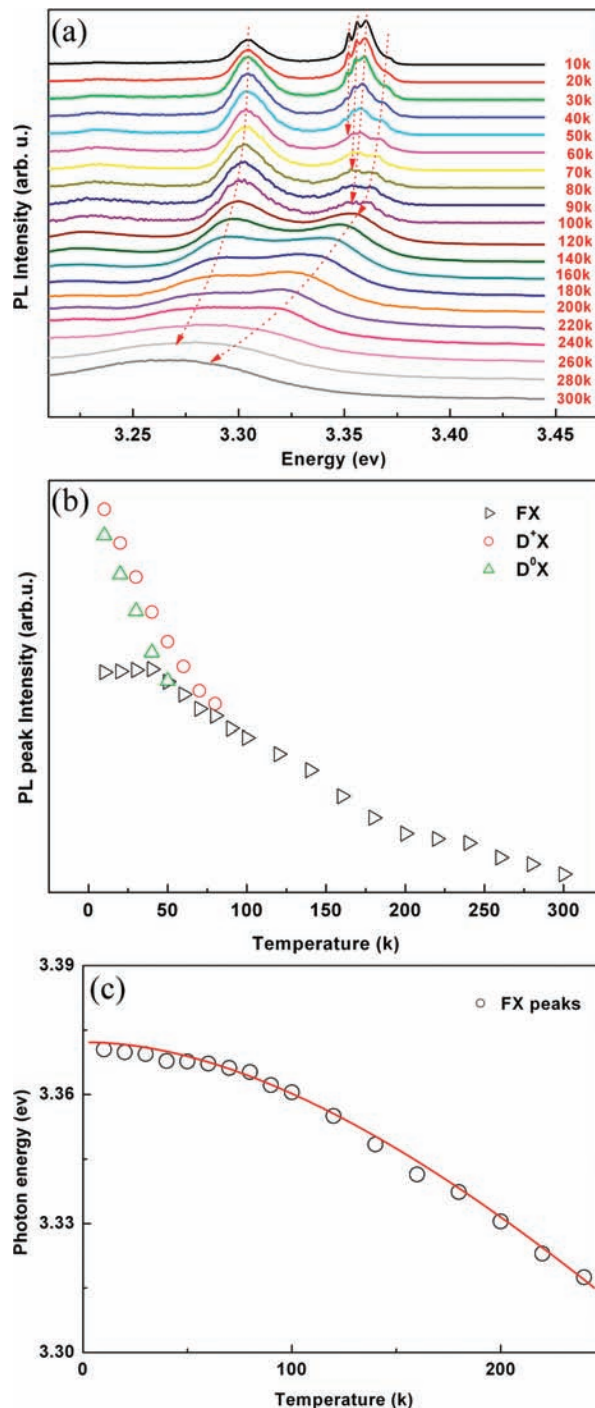
Figure 4. (a) Temperature dependent PL spectral in the range of 10−300K. (b) Temperature dependence of the peak intensities of FX, D⁺X and D⁰X. (c) The temperature dependence of FX peak position. The solid line is the fitting curve of the experimental data by the Varshni's equation.

peaks to D⁰X and ionized donor impurities (D⁺X), respectively. As the temperature increases, the intensity of two peaks decreases due to the thermal dissociation of bound excitons (neutral or ionized) into free ones, as well as the ionization of donor impurities. Meanwhile, the increased number of ionized impurities may increase the chance of excitons binding to D⁺X. This can well explain the slower thermal quenching of the peak at 3.356 eV than the peak at 3.352 eV.

Regarding the shoulder at ∼3.372 eV in Figure 2, to the best of our knowledge, the temperature evolution of this band has never been reported in SnO₂ related materials. The relative

intensity of this shoulder increases as temperature increases (see Figure 4a). We attribute this peak at ~3.372 eV to free exciton (FX) in SnO_2 for the following argument. Figure 4b shows the temperature dependent PL peak intensities of FX, D^+X, and D^0X. We found that the PL intensity of D^0X and D^+X continuously decrease with increasing temperature. But before 40 K, the intensity of the peak at 3.372 eV increases with temperature. This is a very typical behavior for the emission from FX, which is well-known for wide bandgap semiconductors like ZnO.[38,39] As the temperature increases, the bound excitons dissociate and transform into FX. This evidence also supports our assignment of D^0X and D^+X. Although SnO_2 is a dipole forbidden material and the FX emission should not appear in the bulk phase, the nanostructure may break the asymmetry of wave function in SnO_2 and the optical selection rule might be relieved, leading to the appearance of the FX emission. The temperature dependence of bandgap energy of band FX is shown in Figure 4c. The peak energy decreases monotonically as temperature increases, which can be well fitted with the empirical equation describing the semiconductor band gap temperature evolution, viz., Varshni's equation:

$$E(T) = E(0) - \frac{\alpha T^2}{T + \beta}$$

where α, β are constant and $E(0)$ is the band gap at 0 K. As shown in Figure 4c, the curve fits very well with our experiment data. The $E(0)$ obtained from the fitting is 3.372 eV. This provides further evidence that the peak near 3.372 eV originates from the emission of FX.

We notice that the band gap energy of SnO_2 is derived to be 3.502 eV at 10 K by assuming the exciton binding energy to be 130 meV. This value is somewhat different from the claimed ones in other publications.[14,15] The reason for this is unknown at this stage but our data may stimulate further theoretical and experimental explorations; so far, there has been no commonly recognized value of the bandgap of SnO_2.

Conclusions

High quality SnO_2 NWs have been fabricated using a VLS growth method, as has been characterized by XRD, SEM, and TEM. Through high spectral resolution measurement, we have observed rich fine structure in the UV part of the PL spectra. The recombination of donor−acceptor pairs, excitons bound to neutral and ionized donor impurities, as well as optical transitions from free electrons to neutral acceptor impurities have been identified by detailed analysis of temperature- and excitation intensity-dependent PL spectra. In addition, the emission due to the recombination of FX, which does not appear in bulk SnO_2, has also been observed.

References and Notes

(1) Greene, L. E.; Law, M.; Tan, D. H.; Montano, M.; Goldberger, J.; Somorjai, G.; Yang, P. *Nano Lett.* **2005**, *5*, 1231.

(2) Kong, X. Y.; Wang, Z. L. *Appl. Phys. Lett.* **2004**, *84*, 975.

(3) Vayssieres, L. *Adv. Mater.* **2003**, *15*, 464.

(4) Yu, D. P.; Bai, Z. G.; Ding, Y.; Hang, Q. L.; Zhang, H. Z.; Wang, J. J.; Zou, Y. H.; Qian, W.; Xiong, G. C.; Zhou, H. T.; Feng, S. Q. *Appl. Phys. Lett.* **1998**, *72*, 3458.

(5) Morales, A. M.; Lieber, C. M. *Science* **1998**, *279*, 208.

(6) Veglieri, G. S. *Sens. Actuators, B* **1992**, *6*, 239.

(7) Dieguez, A.; Rodriguez, A. R.; Morante, J. R. *Sens. Actuators, B* **1996**, *3*, 1.

(8) Ferrere, S.; Zaban, A.; Gregg, B. A. *J. Phys. Chem. B* **1997**, *101*, 4490.

(9) He, Y. S.; Campbell, J. C.; Murphy, R. C. *J. Mater. Res.* **1993**, *8*, 3131.

(10) Jarzebski, Z. M.; Maraton, J. P. *J. Electrochem. Soc.* **1976**, *123*, 199.

(11) Vasu, V.; Subrahmanyam, A. *Thin Solid Films* **1990**, *193*, 973.

(12) Tsunashima, A. *J. Mater. Sci.* **1986**, *21*, 2731.

(13) Yu, B.; Zhu, C.; Gan, F. *Opt. Mater.* **1997**, *7*, 15.

(14) Arlinghaus, F. *J. Phys. Chem. Solids* **1974**, *35*, 931.

(15) Blattner, G.; Klingshrin, C.; Helbig, R. *Solid State Commun.* **1980**, *33*, 341.

(16) Wang, W. Z.; Xu, C. K.; Wang, G. H.; Liu, Y. K.; Zheng, C. L. *J. Appl. Phys.* **2002**, *92*, 2740.

(17) Xu, C. K.; Zhao, X. L.; Liu, S.; Wang, G. H. *Solid State Commun.* **2003**, *125*, 301.

(18) Liu, Z. Q.; Zhang, D. H.; Han, S.; Li, C.; Tang, T.; Jin, W.; Liu, X. L.; Lei, B.; Zhou, C. W. *Adv. Mater.* **2003**, *15*, 1754.

(19) Hu, J. Q.; Yoshio, B.; Liu, Q. L.; Golberg, D. *Adv. Funct. Mater.* **2003**, *13*, 493.

(20) Cheng, B.; Russel, J. M.; Shi, W. S.; Zhang, L.; Samulski, E. T. *J. Am. Chem. Soc.* **2004**, *126*, 5972.

(21) Pan, Z. W.; Dai, Z. R.; Wang, Z. L. *Science* **2001**, *291*, 1947.

(22) Kong, X. H.; Sun, X. M.; Li, Y. D. *Chem. Lett.* **2003**, *32*, 546.

(23) Dai, Z. R.; Gole, J. L.; Stout, J. D. *J. Phys. Chem. B* **2002**, *106*, 1274.

(24) Wang, Y. L.; Jiang, X. C.; Xia, Y. N. *J. Am. Chem. Soc.* **2003**, *125*, 16176.

(25) Sun, S. H.; Meng, G. W.; Zhang, M. G.; An, X. H.; Wu, G. S.; Zhang, L. D. *J. Phys. D, Appl. Phys.* **2004**, *37*, 409.

(26) Hu, J. Q.; Yoshio, B.; Golberg, D. *Chem. Phys. Lett.* **2003**, *372*, 758.

(27) Chen, R.; Xing, G. Z.; Gao, J.; Zhang, Z.; Wu, T.; Sun, H. D. *Appl. Phys. Lett.* **2009**, *95*, 061908.

(28) Kar, A.; Stroscio, M. A.; Dutta, M.; Kumari, J.; Meyyappan, M. *Appl. Phys. Lett.* **2009**, *94*, 101905.

(29) Zhou, W. C.; Liu, R. B.; Wan, Q.; Zhang, Q. L.; Pan, A. L.; Guo, L.; Zou, B. S. *J. Phys. Chem. C* **2009**, *113*, 1719.

(30) Liu, C. M.; Zu, X. T.; Wei, Q. M.; Wang, L. M. *J. Phys. D: Appl. Phys.* **2006**, *39*, 2494.

(31) Klingshrin, C. *Phys. Stat. Sol.(b)* **1975**, *71*, 547.

(32) Zhang, B. P.; Binh, N. T.; Segawa, Y. *Appl. Phys. Lett.* **2003**, *83*, 1635.

(33) Pluntke, C. H. *Diploma-Thesis*, Erlangen, 1977.

(34) Samson, S. G.; Fonstad, C. *J. Appl. Phys.* **1973**, *44*, 4618.

(35) Kar, A.; Yang, J.; Dutta, M.; Stroscio, M. A.; Kumari, J.; Meyyappan, M. *Nanotechnology* **2009**, *20*, 065704.

(36) Bartolo, B. D.; Powell, R. *Phonon and Resonance in Solids*; Wiley: New York, 1990.

(37) Ahn, C. H.; Mohanta, S. K.; Lee, N. E.; Cho, H. K. *Appl. Phys. Lett.* **2009**, *94*, 261904.

(38) Yang, Y.; Tay, B. K.; Sun, X. W.; Sze, J. Y.; Han, Z. J.; Wang, J. X. *Appl. Phys. Lett.* **2007**, *91*, 071921.

(39) Park, W. I.; Jun, Y. H.; Jung, S. W.; Yi, G. C. *Appl. Phys. Lett.* **2003**, *82*, 964.